JPMTR 063 | 1426
DOI 10.14622/JPMTR-1426
UDC 655 : 681.6 (532.5)

Original scientific paper
Received: 2014-07-15
Accepted: 2015-09-10

Lubrication theory of ink hydrodynamics in the flexographic printing nip

Hans Martin Sauer, Dominik Daume, Edgar Dörsam

Institute of Printing Science and Technology (IDD),
Technische Universität Darmstadt,
Magdalenenstraße 2, D-64289 Darmstadt

E-mail: sauer@idd.tu-darmstadt.de

Abstract

On the base of hydrodynamical lubrication theory, we develop a mathematical model for the ink transfer in a flexographic printing process. When using the specific parameter ranges the model may also be applicable to the offset process. Specifically, we show how our model can be applied to viscous ink flows in the printing nip in presence of elastic printing plates, and how this sets limits to the possible resolution of the printing image. We also discuss the structure of the contact zone between printing plate and the substrate which is determined by the viscous and elastic stresses within the ink layer and the printing form. We also estimate the dynamic pressure profile in the ink during the transfer process. Finally, we discuss the phenomenon of ink seam formation at the rim of a flexographic printed pattern, and viscous finger formation. Explicitly, we show that important parameters, such as the width of an ink seam, the actual nip height, the size of the contact zone, and the ink shear, scale nonlinearly with printing speed. We derive the respective scaling exponents and compare the predictions with printing experiments.

Keywords: flexography, lubrication theory, ink viscosity, ink splitting, viscous fingering

1. Introduction

We present a model for viscous ink flow phenomena between an elastic and structured printing form, and the printing substrate, as it is characteristic for the flexographic process. Our aim is to obtain quantitative predictions for the liquid flows which determine printing resolution, ink squeezing and defect formation, and to understand the role of further parameters such as printing form elasticity, ink viscosity and surface tension, and cylinder diameter. Moreover, we are interested in a more detailed understanding of hydrodynamic nip instabilities such as the famous viscous fingering phenomenon, and of the occasionally appearing ink squeeze at the rim of printed areas in flexographic printed products. The conditions of this annoying phenomenon and the relation to ink viscosity, printing plate elasticity and other printing parameters are still not fully understood, and we expect hydrodynamic theory to give at least some reasonable hint how to remove the problem.

Although printing resolution and quality is crucially depending on the wetting properties of the ink, and the surface free energies of the various materials, the importance of viscous ink flows in the transfer process and specifically at the instant of ink splitting have been emphasized by numerous researchers. Early systematic modelling of ink splitting flows is due to Hopkins (1957). Roller coating processes including defect formation regimes have been studied by Gaskell, Innes and Savage (1998), Varela López et al. (2002), and Varela López and Rosen (2002). The problem of viscous finger formation, or ribbing, has been of continuous interest for several decades, and is usually treated as an analogy of the Saffman-Taylor instability (Saffman and Taylor, 1958). We refer here to the work of Fields and Ashby (1976), of Maher (1985), and of Gingras and Rácz (1989) who emphasized the stochastic nature of finger formation. The importance of the phenomenon for the ink splitting in a printing process has been acknowledged by Behler (1993). Ben Amar (1991) and Lindner and coauthors (Lindner et al., 1999; Lindner, Coussot and Bonn, 2000) have also considered the phenomenon under a more generalized boundary condition, namely in a wedge-shaped rather than a rectangular nip geometry, and for yield stress liquids. An overview is also given in the review of Casademunt (2004). The yield stress aspect is of particular interest for printing inks, and has also been considered by Sauer, Bornemann and Dörsam (2011). The complexity of the problem has been addressed to by the numerical studies of Bohan et al. (2003). We also refer the reader to the PhD thesis of Voss (2002) who presents a systematic collection of the hydrodynamical boundary value problems related to ink splitting. Although we are mainly referring to flexography (Figure 1) in this paper, related instabilities are known to exist also in gravure printing. In flexography, printing ink is supplied to the anilox

roler by a blading system. The anilox roler transports the ink to the protruding parts of the elastic printing plate which is mounted on the plate cylinder. From here the ink is deposited on the printing substrate. This implies lubrication flows in the printing nip, which crucially depend on e.g. the elasticity of the printing plate and on ink viscosity. Bornemann, Sauer and Dörsam (2011), and Bornemann in his PhD thesis (2013), have analyzed viscous flows in a gravure printing nip and show that, quite similar as for flexography, the formation and instability of an ink meniscus are responsible for finger formation, specifically when using printing liquids with extremely low viscosity, which are characteristic for printed electronics. Lubrication approximation of viscous flows has proven to be a fruitful tool here. We shall take this theory as our starting point as well. However, we shall enhance it by discussing the effect of structured and elastic surfaces, which can be deformed by the mechanical and hydrodynamical forces in the nip.

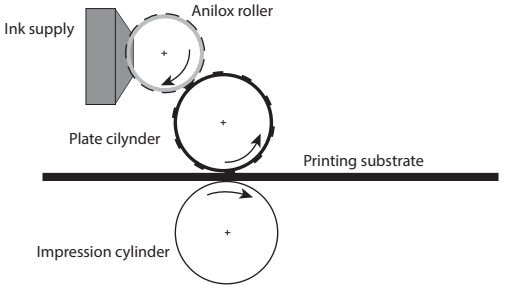

Figure 1: The principal design of a flexographic printing unit

Introducing the model we proceed in five steps: we first discuss a viscous squeeze flow between two parallel plates which are mutually approaching. We then generalize the solution for moderately structured and elastic plates. At this state the model is already capable of describing many aspects of the ink flow between the flexo plate and the substrate, such as details of the ink squeezing at the borders of the plate. In the next step we consider the ink flow between two cylinders, at least one of which has an elastic surface. We identify the stagnation points of the ink flow in the nip. We argue that in a stationary flow the stagnation points define the positions of the ink menisci in the incoming and outgoing wedge between the cylinders. We show that hydrodynamic ink flows give rise to a pressure-driven interaction between incoming and outgoing ink meniscus. We also show how viscous fingering becomes effective here. Although we shall not discuss this point exhaustively, we shall show that our model is in good agreement with the work mentioned above.

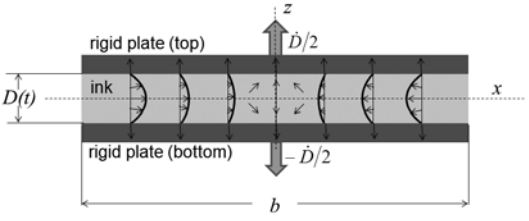

Figure 2: Geometry and flow velocity profile (indicated by the arrows and the bold-printed curves) of a viscous ink between two expanding (or approaching) parallel rigid plates

2. Viscous flow in the gap between two parallel plates which are pressed together or are moving apart

Consider two parallel rectangular plates of width b and length L (oriented in the xy plane, where b corresponds to the x axis) as indicated in Figure 2. We assume that $L >> b$, and we shall finally identify L with the printing width of the plate. The mutual distance $D(t)$ of the plates, where the distance vector is oriented in z-direction perpendicular to the plates, may be time-dependent, but we assume $|D(t)| << b$. The gap between the plates, i.e. the cuboid given by $-b/2 < x < b/2$, $-L/2 < y < L/2$, $-D(t)/2 < z < D(t)/2$ is filled with an ink of viscosity η, which we assume to be Newtonian.

Neglecting inertial versus viscous forces, the flow velocities of the ink in x-, y-, and z-direction are solutions of Stokes equation for incompressible liquids

$$\eta \nabla^2 \vec{v} = \vec{\nabla} p \qquad [1]$$

where η is the dynamic viscosity, ∇ is the del operator, ν is the kinematic viscosity, and p is the pressure, with the incompressibility constraint $\vec{\nabla} \cdot \vec{v} = 0$. The solutions we are interested in are time-dependent due to the boundary conditions given by the moving plates. In the lubrication limit, the viscous shear stress in x- and y-direction is neglected compared to the stress in z-direction, and one obtains

$$\eta \frac{\partial^2 \vec{v}}{\partial z^2} = \vec{\nabla} p \qquad [2]$$

with boundary conditions $v_x = 0$ and $v_z = \pm \dot{D}/2$ at $z = +D(t)/2$ and $z = -D(t)/2$, where $\dot{D} = \partial D / \partial t$. Note here that we do not claim the velocity component v_z and its gradients in z-direction to be negligible, in contrast to Darcy's equation which is suited for cuvette flows as e.g. employed by Saffman and Taylor (1958). This is specifically important for printing inks where elongational ink flows usually cannot be ignored.

Due to the incompressibility, the hydrostatic pressure between the plates satisfies the Laplace equation $\nabla^2 p = 0$. If L is assumed to be very large or infinite,

such that flows and pressure gradients in *y*- direction are negligible, one finds

$$p(x,z,t) = p_0 + \frac{6\eta \dot{D}}{D^3(t)}\left(x^2 - z^2 - \frac{b^2}{4}\right) \qquad [3]$$

where p_0 is the atmospheric pressure outside of the gap, including capillary forces at the ink meniscus. The solution is entirely defined by the condition that the hydrostatic pressure difference towards p_0 should vanish at $|x| \sim b$, with $|x| >> |z|$. By direct inspection one easily shows that the solutions v_x and v_z read as follows

$$v_x(x,z,t) = \frac{6\dot{D}\,x}{D^3}\left(z^2 - \frac{D^2}{4}\right) \qquad [4]$$

$$v_z(x,z,t) = -\frac{6\dot{D}}{D^3}\left(\frac{z^3}{3} - \frac{D^2 z}{4}\right) \qquad [5]$$

and $v_y = 0$. This also satisfies the incompressibility relation $\vec{\nabla}\cdot\vec{v} = 0$. The viscous stress in the printing ink is given by two components of the viscous flow tensor: the shear rate $\gamma_{xz} = 12\dot{D}\,x\,z/D^3$, and the elongational flow rate $\gamma_{zz} = -12\dot{D}\left(z^2 - D^2/4\right)/D^3$. Comparing these components one finds that the shear component is dominant over the elongational one whenever $|x| > |z|$. In the early stage of the plate movement when the distance $D(t)$ is small compared to the plate length b, and when pressure differences are large – hydrostatic pressure p scales as $1/D^3$ – this applies to almost the entire ink volume, except for a narrow strip of width $\approx 2D$ in the very center of the nip. This ratio will be reversed in the later stages of ink splitting when printing plate has substantially lifted from substrate. Hydrostatic pressure will have dropped here. We conclude that the forces acting on the printing plate and the related elastic deformation are a consequence of viscous shear rather than of elongational stress. The lubrication approximation used by Eq. [1] is no longer valid here, and one has to take account of viscous shear in *x*- and *y*-direction. We shall again raise this question in a later section when discussing viscous flows between cylinders (Figure 3).

These above velocity functions can be generalized to plates with a weakly deformed or corrugated instead of a flat surface. This corresponds to a gap of spatially variable width $D(x,y,t)$, with $|dD/dx| << 1$ and $|dD/dy| << 1$:

$$v_x(x,z,t) \approx \int_0^x \frac{6\dot{D}(x',t)\,dx'}{D(x',t)}\left(\frac{z^2}{D^2(x,t)} - \frac{1}{4}\right) \qquad [6]$$

For general $D(x,y,t)$ the integration path should follow a contour in the lateral plane from the reference point 0 to position (x,y). This result is approximate as the flow satisfies the incompressibility condition only up to terms of order of $|dD/dx|\ z^2/D^2$. For the velocity component v_z Eq. [5] still applies, now however with D being dependent on *x*, *y*, and *t*.

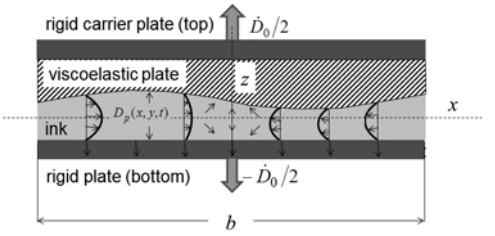

Figure 3: Geometry and ink flow profile between two expanding plates one of which is viscoelastic and deformed by the local hydrodynamic ink pressure

3. Squeeze flow between compressible plates

Our model applies to elastic plates as well. However, we must take account of an additional variability of the gap size $D(x,y,t)$ which is due to the hydrostatic ink pressure p inside the gap. This situation is shown in Figure 3. For the plates we assume a linear viscoelastic compressibility relation

$$D_p = D_0 + \kappa_p\,(p - p_0) - \alpha_p \int_0^t (p(t') - p_0)\,dt' \qquad [7]$$

The time derivative reads

$$\frac{dD_p}{dt} = \dot{D}_0 + \kappa_p \frac{dp}{dt} - \alpha_p\left(p - p_0\right) \qquad [8]$$

where $D_0(t)$ is the gap width in absence of any pressure, $\kappa_p = d_{s,1}/E_1 + d_{z,2}/E_2$ is the plate compressibility; $d_{s,1}$ and $d_{s,2}$ denote the thicknesses of the printing plate and the adhesive bonding tape, respectively, and E_1 and E_2 are the elastic moduli of both materials. Further, a_p describes the viscous creep of the flexo plate in terms of thickness loss per time at unit excess pressure.

Considering the hydrostatic pressure p between the elastic plates Eq. [3] is not applicable any more. The pressure gradients may be obtained from Stokes equation [1] inserting the flow velocity distribution from Eq. [5]. Differentiating this equation three times with respect to z yields the identity

$$\frac{\partial^2 p}{\partial z^2} = \eta \frac{\partial^3 v_z}{\partial z^3} = -\frac{12\eta}{D_p^3}\frac{dD_p}{dt} \qquad [9]$$

with D_p being dependent on *x, y, t,* and *p* according to Eq. [8]. By ink incompressibility p is harmonic in 3D space, i.e. $-\frac{\partial^2 p}{\partial z^2} = \frac{\partial^2 p}{\partial x^2} + \frac{\partial^2 p}{\partial y^2}$, and $p(x,y,z,t)$ is thus fully

determined through the projection of the function p to the x-y-plane, in addition with the viscous boundary conditions at the plates that are already implemented in Eq. [9]. We thus obtain a 2D differential equation for p in the x-y-printing plane, describing viscous ink flow between the deformable plates

$$\left(\frac{\partial^2}{\partial x^2}+\frac{\partial^2}{\partial y^2}\right)p=\frac{12\,\eta\,\kappa_p}{D_0^3}\frac{\partial p}{\partial t}- \frac{24\,\eta\left(\kappa_p\dot{D}_0+\alpha_p D_0\right)}{D_0^4}\left(p-p_0\right)+\frac{12\,\eta\,\dot{D}_0}{D_0^4} \quad [10]$$

We have omitted here terms which are of quadratic order in the compressibility parameter κ_p. Note that, although Eq. [10] is a 2D differential problem, it is capable of describing the full 3D pressure distribution between the plates. We do not assume here that pressure gradients in z-direction are absent. Rather, z-gradients can be reconstructed from Eq. [10] by inserting it into $\nabla^2 p=0$. Further, the ink flow velocities v_x and v_y, (i.e. their average over the liquid layer thickness) can be calculated using Darcy's equation $\vec{v}=-(D^2/12\eta)\vec{\nabla}p$, see e.g. Whitacker (1986).

Squeezed ink volume. By use of Darcy's equation, and by integrating the left hand side of Eq. [10] over the printing area A in the x-y-plane, and over the time history up to the present moment, one can calculate the amount of ink squeezed at the rim ∂A of A up to time t from the beginning of plate movement

$$\int_{-\infty}^{t}\frac{D^3(t')}{12\eta}\int_A\left(\frac{\partial^2}{\partial x^2}+\frac{\partial^2}{\partial y^2}\right)p\,dx\,dy\,dt'= -\int_{-\infty}^{t}D(t')\int_A\left(\frac{\partial v_x}{\partial x}+\frac{\partial v_y}{\partial y}\right)dx\,dy\,dt' = \int_{-\infty}^{t}\oint_{\partial A}D(t')\vec{q}\cdot\vec{v}(t')\,dl\,dt'=V_{sq}^{(A)}(t) \quad [11]$$

Here, $\vec{q}$ is the unit vector in the x-y-plane normal to the rim of the printing plate, and dl is a line segment of that rim. We have replaced the Laplacian of p by the flow velocity according to Darcy's law, and then applied Gauss' integral theorem. Calculating the amount of ink squeeze for an elastic printing plate is now possible according the following procedure: solve Eq. [8] for the specific plate–substrate distance and the boundaries of the printing area as being defined by the printing layout, take the Laplacian of the pressure, and obtain its integral according to Eq. [11].

Mathematically Eq. [10] corresponds to a standard 2D-heat diffusion equation, where the pressure p has the role of the temperature. We refer the reader to the textbook of Landau and Lifshitz (1970) where the physical content of the coefficients in such equations is thoroughly discussed. From this analogy, we can define macroscopic parameters which determine the overall behavior of the system such as a constant of pressure relaxation, the ink squeeze length, and the power dissipation endowed with viscous ink shear.

For sake of simplicity we omit the creep constant a_p in the sequel but emphasize that it could easily be integrated by a simple redefinition of the coefficients in the differential equation.

Consider the case that the two plates have been approaching each other so that some hydrostatic pressure has developed in the gap. When the plate movement is interrupted at time t_0, i.e. if $dD_0/dt = 0$ for $t > t_0$ Eq. [8] reduces to

$$\left(\frac{\partial^2}{\partial x^2}+\frac{\partial^2}{\partial y^2}\right)p=\frac{12\,\eta\,\kappa_p}{D_0^3}\frac{\partial p}{\partial t} \quad [12]$$

from t_0 on. The pressure between the plates is now described by the strongly simplified diffusion Equation [12]. The pressure and its gradients do not disappear immediately at $t = t_0$, but pressure relaxation will take some time depending on the spatial pressure distribution between the plates and specifically at the edges. The key observation is that ink flow is characterized by some kind of diffusion constant

$$\Lambda_p=\frac{D_0^3}{12\,\eta\,\kappa_p} \quad [13]$$

During the period of relaxation there is an ink flow along the gradient direction of the pressure. This specifically applies to the rims of the printing area of plates, where ink is squeezed out.

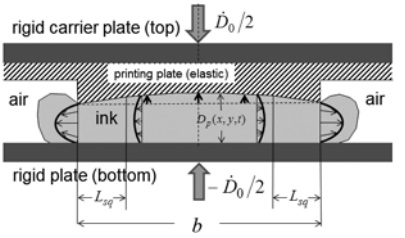

Figure 4: The squeezing of ink at the rim of a printing element of width b on the printing plate with the flow profiles; the pressure-related elastic deformation of the printing form is indicated by the bold printed arrows

When b is the length of the plate in printing direction, or of the structure element on a printing form, we can estimate the time span in which ink will still be squeezed out at the rim after t_0

$$\Delta t_{sq}\propto\frac{b^2}{\Lambda_p}=\frac{12\,\eta\,d_s}{D_0^3\,E}b^2 \quad [14]$$

The ink forms a more or less pronounced seam, or halo, at the rim as indicated in Figure 4, with printing results as shown in Figure 5.

Consider now the case that the printing plate is approaching the substrate with small but constant velocity dD_0/dt. The protruding elements on the printing plate, covered with ink, will come into contact with the printing substrate at some point. After contact the ink pressure will start to increase more or less constantly in time throughout the printing area, except for a narrow seam along the rim of the protruding element. The pressure here will cease to rise accordingly, as ink is continuously escaping sidewise beyond the rim. We denote the width of the zone where this ink squeeze is substantial as the squeeze length L_{sq}. It can be determined from the coefficient of the steady-state diffusion problem, and depends on dD_0/dt as follows

$$L_{sq} = \frac{D_0^2}{\sqrt{24\eta\kappa_p \dot{D}_0}} \qquad [15]$$

This width essentially determines a limit for the resolution of the flexo printing process imposed by viscous ink flows. The aim of accurate printing is, of course, to keep this length small.

Figure 5: Typical seam or "halo" of a flexo printed pattern: the ink has been squeezed and has been deposited in the seam at the rim of the printed pattern; depositing ink within the intended areas has failed: only residuals of the ink have remained, and form a labyrinth-shaped structure

4. Squeeze flow between elastic rotating cylinders

Cylindrical surfaces can be approximated by parabolic ones as far as the nip region is concerned. The gap width (in absence of elastic deformation) is

$$D_0(x,y,t) \propto D_n + \frac{1}{2r_n}\left(x - v_p t\right)^2 \qquad [16]$$

where D_n is the minimum distance between printing plate surface and substrate in the nip, $\frac{1}{r_n} = \frac{1}{R_p} + \frac{1}{R_i}$ is the total surface curvature in the nip, defined by the radii R_p of the printing and R_i of the impression cylinder, and v_p is the printing velocity. By the analogous derivation as described in Eq. [10] one can again obtain an equation for the ink pressure as measured by an observer attached to the substrate who is moving through the nip with printing velocity $-v_p$:

$$\left(\frac{\partial^2}{\partial x^2} + \frac{\partial^2}{\partial y^2}\right) p = \frac{96\,\eta\, r_n^3}{\left(\lambda_n^2(p) + (x - v_p t)^2\right)^3} \times \left(\kappa_p \frac{\partial p}{\partial t} + \kappa_p v_p \frac{\partial p}{\partial x} + \frac{4\,\kappa_p v_p (x - v_p t)}{\lambda_n^2(p) + (x - v_p t)^2}\right)\left(p - p_0\right) - \frac{v_p (x - v_p t)}{r_n} \qquad [17]$$

where

$$\lambda_n(p) = \sqrt{2 r_n (D_n + \kappa_p (p - p_0))} \qquad [18]$$

is the pressure-corrected nip length, i.e. the width of the contact zone of printing plate and substrate where a substantial shear flow is created. Note also that the right hand side of Eq. [17] is substantially distinct from 0 in a range of width

$$\lambda_n = \sqrt{2 r_n D_n} \qquad [19]$$

in the nip. In the sequel, this length will essentially have the role of b in Eqs. [3] and [12]. We call this the effective nip length. From the observation that according to Eq. [19] the effective nip length $\lambda_n >> D_n$ is much larger than its width, and considering that elongational stress in the ink is dominant only within the small range $|x| < D_n$, we also conclude that viscous shear and not elongational stress in the ink is dominant for hydrostatic pressure formation and for printing form deformation. As the width is a function of the ink pressure, the squeeze problem now becomes essentially a nonlinear one. Nevertheless, the solutions of this equation have a number of general properties. In the case of hard surfaces ($\kappa_p = 0$), and assuming a steady-state process, the pressure equation can be integrated, yielding the time-independent solution

$$p(x) = p_0 + p_{visc}\left(\zeta(x/\lambda_n) - \frac{x}{x_m}\zeta(x_m/\lambda_n)\right) \qquad [20]$$

with $p_{visc} = 12\eta v_p r_n^2 / \lambda_n^3$
and the dimensionless function $\zeta(x) = \frac{x}{1+x^2} + \arctan x$.

We have assumed here that the pressure at the ink menisci on both sides of the nip (i.e. $p(x)$ at $x = -x_m$ and $x = x_m$ equals the atmospheric air pressure p_0.

For $|x_m| > x > -|x_m|$ the solution predicts that a point on the substrate which is moving through the nip first experiences a pressure maximum well above the air pressure. The pressure then drops to a minimum situated on the outgoing half of the nip. This pressure minimum is responsible for the back flow of ink from the diverging surfaces to the nip.

Assuming parameters here as listed in Table 1, however, clearly indicates that the hard-cylinder case strongly overestimates the pressure, and that viscous ink flows in the nip cause a significant increase of the nip length $\lambda_n(p)$ by the exerted hydrostatic pressure according to Eq. [18].

Moreover, viscous forces give rise to a small but finite mechanical torque acting on the printing cylinder. This torque is directed such as to hamper the rotation of the cylinder.

In order to obtain a more realistic estimate on the length $\lambda_n(p)$ we consider its value at the pressure maximum p_{visc} and insert this into Eq. [18]. Resolving this equation for $\lambda_n(p)$, and provided that the printing velocity v_p satisfies $|v_p| >> v_{sq} = \frac{D_n^2}{24\pi\eta\kappa_p}\sqrt{2D_n/r_n}$, one obtains a nip length scaling with the printing velocity v_p

$$\lambda_n(p_{visc}) \propto \left(24 r_n^3 \kappa_p \eta |v_p|\right)^{0.2} \qquad [21]$$

Velocity v_{sq} essentially is the typical squeeze flow velocity of the ink and of order of mm/s. Eq. [21] is a remarkable result as it shows that the nip length does no longer depend on the initial nip height D_n, and is much larger than the value predicted from hard cylinders.

Using the parameter set assumed in Table 1, we obtain values of approximately 2 mm instead of 600 μm. The nip length is therefore determined by the equilibrium of elastic and viscous forces in the nip as created by the ink flow. Inserting this result into Eq. [18] we can conclude that there are scaling relations of further quantities as well. Pressure scales as $p - p_0 \propto v_p^{0.4}$,

the average nip height satisfies
$D(p_{visc}) \propto \sqrt{2 r_n \kappa_p p_{visc}} \propto v_p^{0.2}$,

and the squeeze time is $\Delta t_{sq} \approx \lambda_n(p_{visc})/v_p \propto v_p^{-0.8}$.

Finally, using again Darcy's equation, we obtain the scaling law for the squeeze velocity
$v_{sq} = \left|-(D^2(p_{visc})/12\eta)\,\vec{\nabla}p\right| \propto v_p^{0.6}$.

We can further estimate the ink displacement $W(v_p) \propto v_{sq}\,\Delta t_{sq}$ caused by the squeeze flow.

$$W(v_p) = v_{sq}\,\Delta t_{sq} \propto \frac{D^2(p_{visc})}{12\eta}\,\frac{p - p_0}{\lambda_n(p)}\,\Delta t_{sq} \propto \frac{\left(v_p^{0.2}\right)^2 v_p^{0.4}}{v_p^{0.2}} v_p^{-0.8} = v_p^{-0.2} \qquad [22]$$

Eq. [22] implies that ink squeeze is reduced with increasing printing velocity with a specific exponent of −0.2.

Table 1: Typical orders of magnitude of the relevant parameters for a flexo printing process

Parameter	Symbol	Equation	Typical values
Ink viscosity	η	[1]	20 mPa·s
Thickness of the flexo plate & adhesive tape	d_s	[8]	2 mm
Young modulus of the flexo plate	E	[8]	20−100 MPa
Compressibility constant	κ_p	[8]	$0.2-1\cdot10^{-10}$ m³/N
Pressure diffusivity	L_p	[13]	0.01−0.1 m²/s
Squeeze time at b = 600 μm	Δt_{sq}	[14]	0.1−10 s
Squeeze length	L_{sq}	[15]	20−100 μm
Nip height	D_n	[16]	1−2 μm
Static nip length for hard cylinders (r_n = 10 cm)	λ_n	[19]	600 μm
Dynamic nip length for elastic cylinders (r_n = 10 cm) with self-consistent calculation	$\lambda_n(p)$	[18]	2 mm

Table 2: Overview over flexo printing parameters X and length scales which depend on the printing velocity v_p according to $X \propto v_p^k$ and the respective exponents k; the increase or decrease of X that is predicted if v_p is doubled is indicated as well

Parameter X	Symbol	Exponent k	Expected relative change at doubled printing speed
Nip length	$\lambda_n(p_{visc})$	+0.2	+15 %
Nip pressure	p_{visc}	+0.4	+32 %
Effective nip height	$D(p_{visc})$	+0.2	+15 %
Ink squeeze time	Δt_{sq}	−0.8	−53 %
Ink squeeze velocity	v_{sq}	+0.6	+52 %
Ink shear	$\propto v_{sq} / D(p_{visc})$	+0.4	+32 %
Ink seam width	$W(v_p)$	−0.2	−13 %

Considering a specific flexo printing job this means that seam formation at the rim of printed patterns should reduce by 13 % when accelerating the printing press by a factor of 2. Further tendencies are summarized in Table 2. This prediction can be checked experimentally by examination of printed samples as we shall show now.

Figure 6 shows scans of flexo printed samples with specific defects that will be discussed using the above model. Arrays of full-area rectangles of 30 × 15 mm in size were printed on coated paper (IGEPA Maxisatin, 90 g/m²) at different printing speeds between 20 and 160 m/min using a Gallus RCS 330 printing press. As printing ink, water based gravure/flexo ink type 8/110305 WD from Ruco (A. M. Ramp & Co. GmbH, Eppstein, Germany) was used and diluted with 50 vol. % of deionized water. The anilox roler (Zecher GmbH, Paderborn, Germany, standard Cr_2O_3 ceramic surface on aluminium) had a raster width of 130 lines per cm and a transfer volume of 13.2 ml/m². The flexo plate was made of nyloflex FAH digital, with a hardness of 60 ShA, and 1.14 mm of thickness.

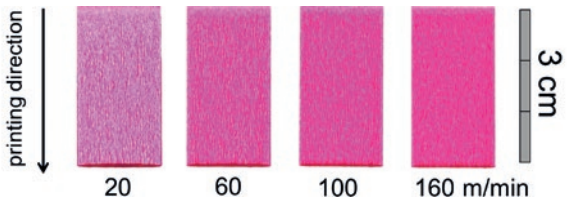

Figure 6: Flexo printed rectangles created with printing velocities of 20, 60, 100, and 160 m/min; the rectangles show a pronounced viscous fingering (ribbing), and ink seam at the edge in forward direction (i.e. at their bottom); the width of this rim scales with the printing velocity v_p

The printed rectangles exhibit two peculiar features: viscous finger formation, and ink squeezing. Ink squeezing resulted in a dense ink seam at the rectangle's border situated at the printing end. Here, the ink conducted in the nip zone is released from the rear edge of the printing area on the flexo plate, and deposited on the substrate. The width W (measured by digital evaluation of a 600 dpi scan of the printed samples, see Figure 6) of this seam is therefore essentially equal to the width $2\lambda_n(p_{visc})$ of the nip zone, or at least proportional to this length scale.

In the considered range of printing velocities we obtained seams of 0.5 to 0.7 mm in width. Plotting these values versus printing speed v_p we are thus able to check the scaling law implied by Eq. [21], which predicts that $\lambda_n(p_{visc}) \propto v_p^k$, with an exponent $k = -0.2$. Evaluating our printed samples we find that $k = -0.158 \pm 0.059$ which is indicated as the dash-dotted line in the logarithmic plot in Figure 7.

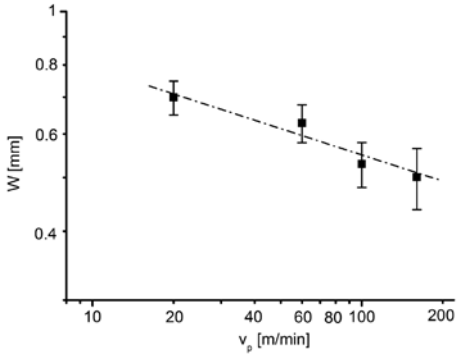

Figure 7: The width W of the seam as a function of printing velocity; the decrease of W corresponds to a scaling exponent $k = -0.158 \pm 0.059$ (dash-dotted line)

5. Stagnation points of viscous nip flow and how they affect the ink transfer

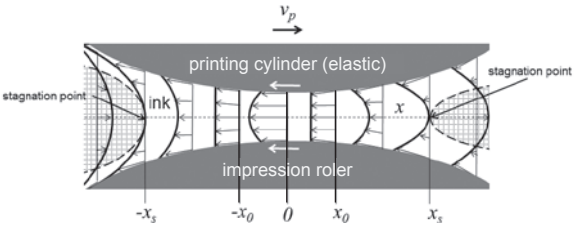

Figure 8: Ink flow velocity in the nip between two rotating cylinders, indicated by arrows and bold-printed curves; in the center region of the nip ($-x_0 < x < x_0$) the velocity of the ink exceeds the revolution speed of the cylinders (unless $x_0 = 0$), for $x > x_0$, and for $x < -x_0$, the ink flow is retarded in the middle between the cylinders and comes to rest the stagnation points $x = x_s$ and at $x = -x_s$; ink in the cross-hatched area never passes the nip but is trapped in circulating vortices before and after the nip

Ink squeezing is the consequence of a viscous ink flow in the microscopic gap between flexo plate and substrate, and here, we therefore have to consider ink velocity profile in the nip, using Eq. [6]. This equation describes an excess in flow velocity in the center between the two surfaces, with a Hagen-Poseuille type velocity profile. This excess flow terminates at two stagnation points in a distance x_s in front of and behind the nip. This is depicted in Figure 8. The ink is apparently at rest here, i.e. $v_x(\pm x_s) = 0$. On the cylinder surfaces, the ink velocity is identical to v_p. In contrast, the ink velocity in the center of the nip, i.e. at $z = 0$, *is*:

$$v_x(x, z=0) = v_p - \frac{3}{2}\int_{x_0}^{x} \frac{\dot{D}_p(x')}{D_p(x')}dx' = v_p + \frac{3v_p}{2}\log\frac{x_0^2+\lambda_n^2}{x^2+\lambda_n^2} + O(\dot{p}) \qquad [23]$$

The point x_0 corresponds to the position along the x axis where $v_x(x) = v_p$, and is an arbitrary parameter of the solution.

The ink velocity approaches zero at positions $x = \pm x_s$, with

$$x_s \approx \pm\sqrt{1.9477\,x_0^2 + 0.9477\,\lambda_n^2} \qquad [24]$$

These are the stagnation points of the ink flow. Ink outside these points, i.e. at positions $|x| > |x_s|$ will never pass through the nip. These ink portions will first approach the nip up to some minimum distance, but then reverse their movement in opposite direction. For this reason, the ink menisci located at $x = \pm x_m$ must coincide with the stagnation points in a steady-state situation, and the ink pressure must equal the atmospheric, in addition to the capillary pressure. In other words, $x_s = x_m$ holds here. The important point is that there is more than one solution of the hydrodynamic problem, and that these solutions are distinct in the position x_0 of shear-free flow, and in the stagnation points. The ink flow therefore is in an approximately indifferent equilibrium, and the flow and pressure distribution depend on the quantity of printing ink supplied to the nip, and on further forces such as capillary pressure. Moreover, the stagnation points, and therefore the menisci on both sides of the nip, are in mutual interaction. They cannot be shifted independently. Supplying more ink on the incoming side of the nip will move the stagnation points further apart from the nip. This, in turn, will increase the Poseuille pressure, and squeeze additional ink portions through the nip, thereby widening the opening between the elastic printing plate surface and the substrate. This has an important consequence with respect to ink transfer: providing more ink to the printing plate by the anilox roller will also increase the transferred ink volume on the printing plate as the stagnation points of the ink flow will move outwards. One further aspect concerns the formation of possible ghost images: in spite of the intense shear of the ink in the nip the amount of ink deposited on the substrate depends on the excess ink that resides in the menisci of the nip since former contacts with substrate or anilox roller, as the excess ink will contribute to later ink transfer events.

6. Viscous finger formation

We now consider the linear stability of a straight ink meniscus. As there is apparently more than one solution possible, distinguished by x_0, we take account of capillary forces at the meniscus in order to decide which of the solutions is preferred by the surface forces, and whether this corresponds to a straight meniscus. We anticipate that the latter is not the case, specifically for the outgoing nip. Rather, the formation of finger-like patterns, viscous fingering, is usually observed. This is related to the Saffman-Taylor instability which is observed at retracting liquid surfaces. We shall not discuss this here in detail, and we restrict to cylinders with hard surfaces. Our aim here is to demonstrate how viscous fingering instabilities principally appear in our model.

$$\left.\frac{\partial\, p(x)}{\partial x_m}\right|_x = p_{visk}\,\frac{x}{x_m^2}\left[\frac{x_m\,\lambda_n\left(x_m^2-\lambda_n^2\right)}{\left(x_m^2+\lambda_n^2\right)^2} + \arctan\frac{x_m}{\lambda_n}\right] = p_{visk}\,\frac{x}{x_m^2}\left[0.7586 + O\left(\frac{x_0}{\lambda_n}\right)^2\right] \qquad [25]$$

Taking the derivative of Eq. [20] with respect to the position x_m of the ink meniscus we find that at a given position x, with $-x_m < x < 0$ on the outgoing side behind the meniscus the ink pressure $p(x)$ is raising as the meniscus retracts towards the nip.

When considering elastic printing plates, one has, of course, to take the derivative of the full solution of Eq. [17] instead. As the derivative Eq. [24] is a negative on the outgoing side of the nip the solution cannot be stable: small fluctuations $\Delta x_m(y) = x_m(y) - x_{m,0}$ of the meniscus position $x_m(y)$ from the average position $x_{m,0}$ across the width of the printing plate will cause ink to be shifted from positions where the meniscus is retracting to positions where it is expanding. When we equilibrate these pressure fluctuations by the excess of surface energy related to the deformation of the meniscus as is given by

$$p_L = -\sigma \frac{\partial^2 x_m}{\partial y^2} \qquad [26]$$

with σ as the surface tension of the ink, we obtain that periodic instabilities are possible for wavelengths larger than

$$\lambda_{\min}^{V.F.} = \sqrt{\frac{\sigma \lambda_n^3 x_{m,0}}{9.103 \eta v_p r_n^2}} \propto D_n \sqrt{\frac{\sigma}{4 \eta v_p}} \qquad [27]$$

This is, up to minor numerical corrections, the well-known result from Saffman and Taylor (1958), and of the other authors cited above. In this manner it is possible to study viscous fingering phenomena between curved and elastic surfaces from solutions of the pressure equation [17], using capillary pressure at the meniscus as a boundary condition.

7. Conclusions

The specific benefit of our model is the following. It reduces the complex 3D hydrodynamic problem of ink splitting, at least under the assumptions of lubrication theory, to a still challenging but much better accessible 2D scalar potential problem. With respect to flexography, moreover, an essentially linear regime of this mathematical model is relevant, rendering many interesting questions into the range of analytic studies: the effect and significance of the elastic deformation of the printing form, the systematical analysis of squeeze flows and ink splitting in the nip, on full-tone as well as on structured printing forms. Providing the surface profile of a printing form one can further define the complete boundary value problem for the calculation of pressure distribution, ink flows, and the ink distribution on the substrate. This could be of great help when designing high-resolution flexographic printing forms, as it is able to predict the ink flows as a function of the shape of the printing form.

Acknowledgements

We would like to appreciate the funding of this work by the German Federal Ministry of Research and Education (BMBF) under grant no. 13N10298 (NanoPEP).

Literature

Behler, H., 1993. *Die Randstruktur von Druckpunkten – Eine experimentelle Untersuchung der Farbspaltungsströmung*, PhD thesis, TU Darmstadt.

Ben Amar, M., 1991. Viscous fingering ia a wedge, *Physical Review A*, 44(6), pp. 3673–3685.

Bohan, M.F.J., Fox, I.J., Claypole, T.C. and Gethin, D.T., 2003. Influence of non-Newtonian fluids on the performance of a soft elastohydrodynamic lubrication contact with surface roughness, *Proceedings of the Institution of Mechanical Engineers, Part J: Journal of Engineering Tribology*, 217, pp. 447–459.

Bornemann, N., Sauer, H.M. and Dörsam, E., 2011. Gravure printed ultrathin layers of small-molecule semiconductors on glass, *Journal of Imaging Sciences Technology*, 55(4), pp. 040201-1–040201-8.

Bornemann, N., 2013. *Characterization and Investigation of Large-Area, Ultra-Thin Gravure Printed Layers*, PhD thesis, TU Darmstadt [online]. Available at: <http://tuprints.ulb.tu-darmstadt.de/id/eprint/3847> [Accessed 10 September 2015].

Casademunt, J., 2004. Viscous fingering as a paradigm of interfacial pattern formation: recent results and new challenges, *Chaos*, 14(3), pp. 809–824.

Fields, R.J. and Ashby, M.F., 1976. Finger-like crack growth in solids and liquids, *Philosophical Magazine*, 33(1), pp. 33–48.

Gaskell, P.H., Innes, G.E. and Savage, M.D., 1998. An experimental investigation of meniscus roll coating, *Journal of Fluid Mechanics,* 355, pp. 17–44.

Gingras, M.J.P. and Rácz, Z., 1989. Noise and the linear stability analysis of viscous fingering, *Physical Review A*, 40(10), p. 5960.

Hopkins, M.R., 1957. Viscous flow between rotating cylinders and sheet moving between them, *British Journal of Applied Phys*ics, 8(11), p. 442.

Landau, L.D. and Lifshitz, E.M., 1970. *Theory of Elasticity,* 2nd ed. Oxford: Pergamon Press.

Lindner, A., Bonn, D., Ben Amar, M., Meunier, J. and Kellay, H., 1999. Controlling viscous fingering. *Europhysics News,* 30(3), pp. 77–78.

Lindner, A., Coussot, P. and Bonn, D., 2000. Viscous fingering in a yield stress fluid, *Physical Review Letters,* 85(2), pp. 314–317.

Maher, J.V., 1985. Development of viscous fingering patterns, *Physical Review Letters,* 54(14), p. 1498.

Saffman, P.G. and Taylor, G., 1958. The penetration of a fluid into porous medium or Hele-Shaw cell containig a more viscous fluid, *Proceedings of the Royal Society of London, Ser. A*, 245(1242), pp. 312–329.

Sauer, H.M., Bornemann, N. and Dörsam, E., 2011. Viscous fingering in functional flexo printing: an inevitable bug? In: *Large-area, Organic & Printed Electronics Convention (LOPE-C)*, Organic and Printed Electronics Association, Frankfurt, Germany.

Varela López, F., Pauchard, L., Rosen, M. and Rabaud, R., 2002. Non-Newtonian effects on ribbing instability threshold, *Journal of Non-Newtonian Fluid Mech*anics, 103, pp. 123–139.

Varela López, F. and Rosen, M., 2002. Rheological effects in roll coating of paints, *Latin American Applied Research*, 32, pp. 247–252.

Voss, C., 2002. *Analytische Modellierung, experimentelle Untersuchung und dreidimensionale Gitter-Boltzmann-Simulation der quasistatischen und instabilen Farbspaltung*, PhD thesis, Universität Gesamthochschule Wuppertal.

Whitacker, S., 1986. Flow in porous media I: A theoretical derivation of Darcy's law, *Transport in Porous Media*, 1(1), pp. 3.25.